Natural Wave Propagation in Mine Environments

Martine Liénard and Pierre Degauque, *Member, IEEE*

***Abstract*—Theoretical and experimental aspects of the natural propagation of high-frequency waves in mines are presented. A narrow-band and a wide-band analysis have been carried out to determine the most important characteristics of the channel such as the longitudinal attenuation, the coherence bandwidth, and the delay spread of the impulse response in the various areas of an underground mine. The basic principle of a localization of a mobile has also been checked by determining the direction of arrival of the waves.**

***Index Terms*—Delay spread, electromagnetic (EM) wave propagation, mining industry, propagation in tunnels.**

I. Introduction

THE propagation of electromagnetic (EM) waves in mining environments has been extensively studied during the last 30 years and the contribution of James R. Wait to this field was outstanding. Underground mines are extensive labyrinths that employ many people working over many square kilometers and communications are necessary to achieve coordinated tasks. The main emphasis of both the theoretical and experimental approach concerned the field attenuation versus the distance between the transmitter and the receiver in order to optimize the choice of the transmitting frequency for the analog transceiver. Furthermore, in such confined areas, various solutions have been proposed to get a wide radio coverage and, before describing the more recent research in this field and the new applications, it may be of interest to recall very briefly the various options to transmit a signal. Let us first consider a transmission in the low frequency range, typically on the order of 10 MHz. In an empty mine entry, the signal strength is often not useable for distances greater than about 30 m. Nevertheless, in most practical cases, electric cables, pipes, etc., are running in the galleries and one can expect that the magnetic field radiated by a loop transmitting antenna will couple to these wires exciting thus, guided modes propagating with a low attenuation. As mentioned by Emslie *et al.* [1], mines with electrical rail haulage almost always use carrier frequency communication, the transmission line being formed by the trolley wires and the rails. To avoid the effect of many bridging loads, branches, and unterminated line ends, a dedicated auxiliary wire can be deployed in the tunnel supporting a so-called monofilar mode, propagating like a coaxial or TEM mode. Another communication technique developed by Delogne *et al.* [2] utilizes a two-wire transmission line that can be suspended from the upper wall. The key step of this system is to convert the monofilar mode to a bifilar mode, which is less attenuated because the return current flows in the second wire rather than through the surrounding rock. Mode converters are inserted in one line but this mode conversion may also be achieved without any additional device due to the random change in the tunnel cross section. The propagation constants of these various modes and the field distribution in the gallery have been widely studied by James R. Wait *et al.* [3], [4].

An improvement of this technique appeared with the introduction of leaky coaxial cable. The continuous leakage through the outer shield of the cable allows a coupling between the transmission modes inside the cable and the modes supported by the external region. For frequencies up to 100 MHz, an inexpensive solution is to use a loosely braided coaxial cable. In this case, the sheath is characterized by a transfer impedance and its value is a tradeoff between the longitudinal attenuation of the cable and the coupling loss between the coaxial mode and the external modes. A general formulation accounting for both the ohmic losses in the tunnel and a thin lossy film layer on the outer surface of the dielectric jacket of the cable has been proposed by Wait *et al.* [5]–[7]. It appears that, for typical cable parameters, the optimum frequency is found to be in the range from 2 to 10 MHz. More recently, the increasing demand of the coverage of road and railway tunnels for digital phone, i.e., in a band extending from 900 MHz to 2.1 GHz, gave rise to the development of new types of radiating cables. In this case, transverse, or inclined slots are distributed on their outer shield. The distance between each slot being on the same order of magnitude as the wavelength, the cable behaves as a long array of equivalent magnetic dipoles. The radiation of such a cable is described in [8], for example, for an application in a road tunnel and in [9] for a digital communication in mine access galleries. A review of various aspects of EM wave propagation in tunnels can also be found in [10].

However, the geometrical configuration of a mine is not limited to a succession of interconnected galleries and the exploitation is now essentially based on room and pillars techniques. Typically, thick ore deposits are exploited by means of heavy diggers in a very changing area that has a complicated pattern and the implementation of radiating cables is out of question. The only possibility is to use the natural propagation of the waves owing to the multiple reflections, diffraction and diffusion on the walls. In this case, preliminary experiments have shown that the transmitting frequency must be greater than few hundred megahertz to cover an approximate square area, 100-m side. In order to improve the productivity and the safety conditions in underground mines operations, systems of communication and localization of mine workers and mobile equipment have to be developed. Furthermore, data sent by the various equipment, sensors, and actuators in the mine monitoring system must use an efficient and reliable network and a wireless link is an attractive option. The objective of this paper is

Manuscript received June 25, 1999; revised February 24, 2000. This work was supported in part by the European Community, BRITE Project MICOLOS.

The authors are with the Electronics Department, University of Lille, 59 655 Villeneuve d'Ascq Cedex, France (e-mail: Martine.Lienard@univ-lille1.fr).

Publisher Item Identifier S 0018-926X(00)09382-0.

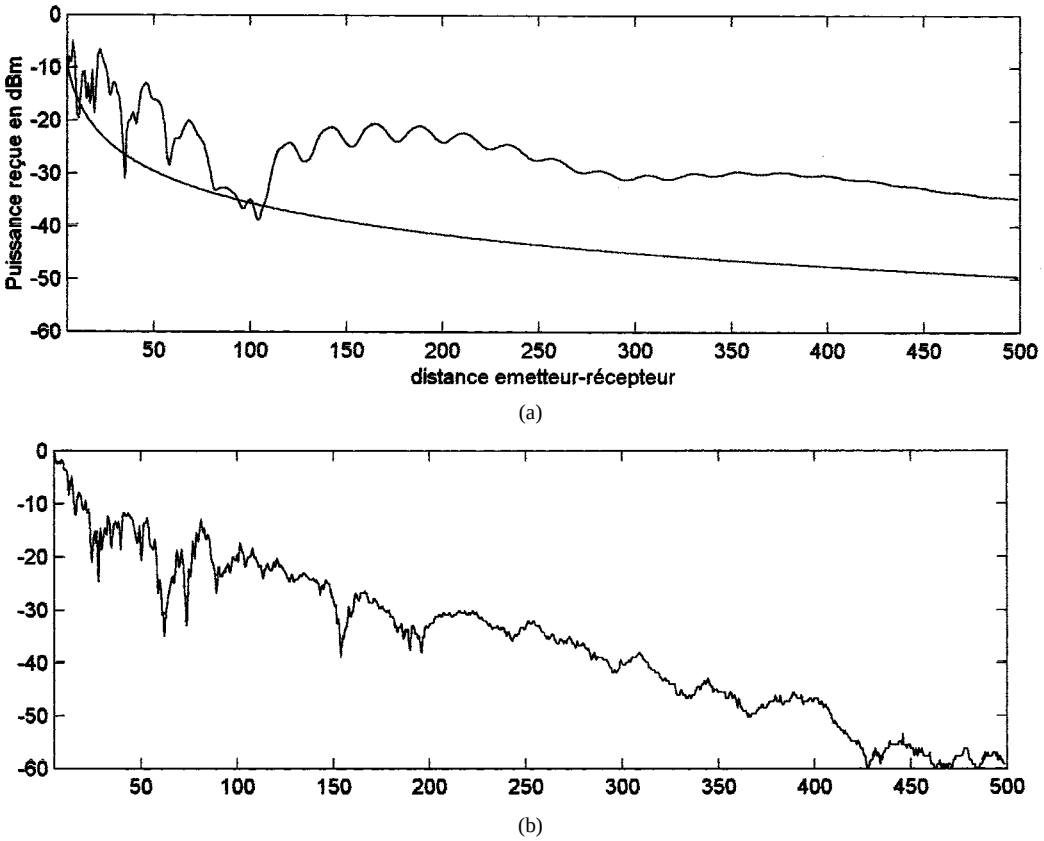

Fig. 1. Variation of the received power in a mine gallery versus the distance transmitter-receiver at 450 MHz. Curve (a) Theoretical results, the continuously decreasing curve corresponding to the contribution of the direct path. Curve (b) Experimental results on 500 m.

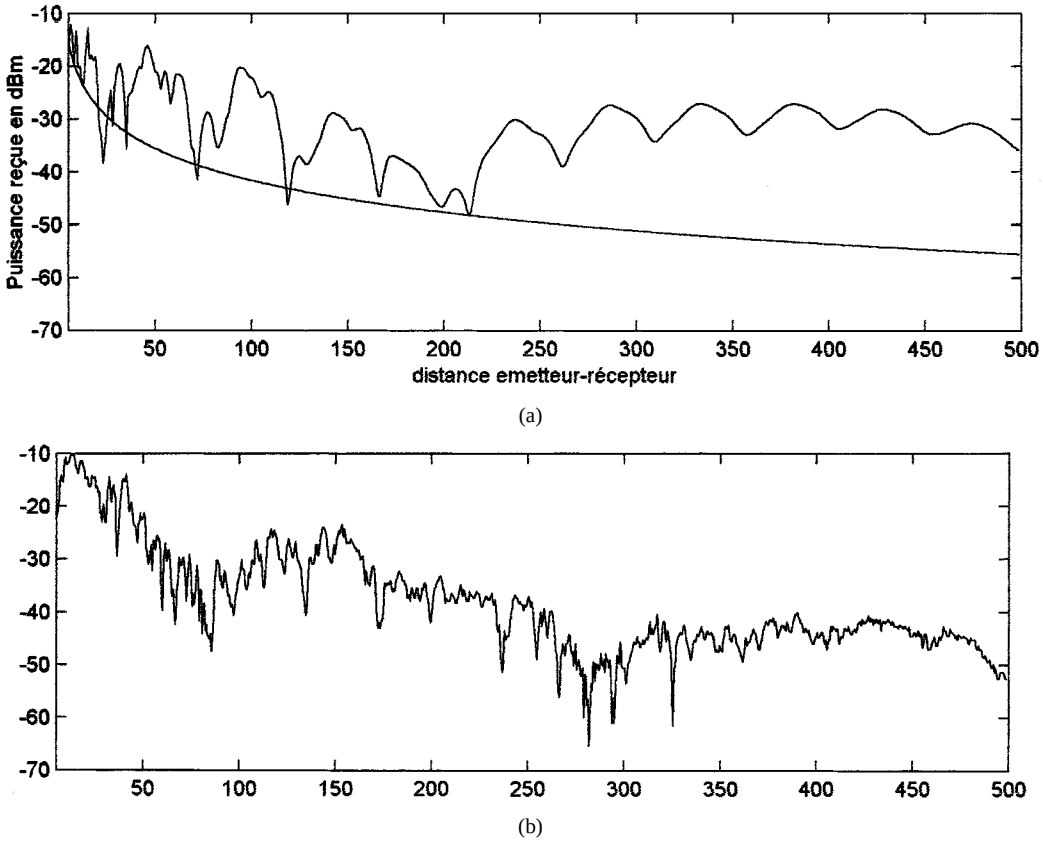

Fig. 2. Same as in Fig. 1, but at 900 MHz.

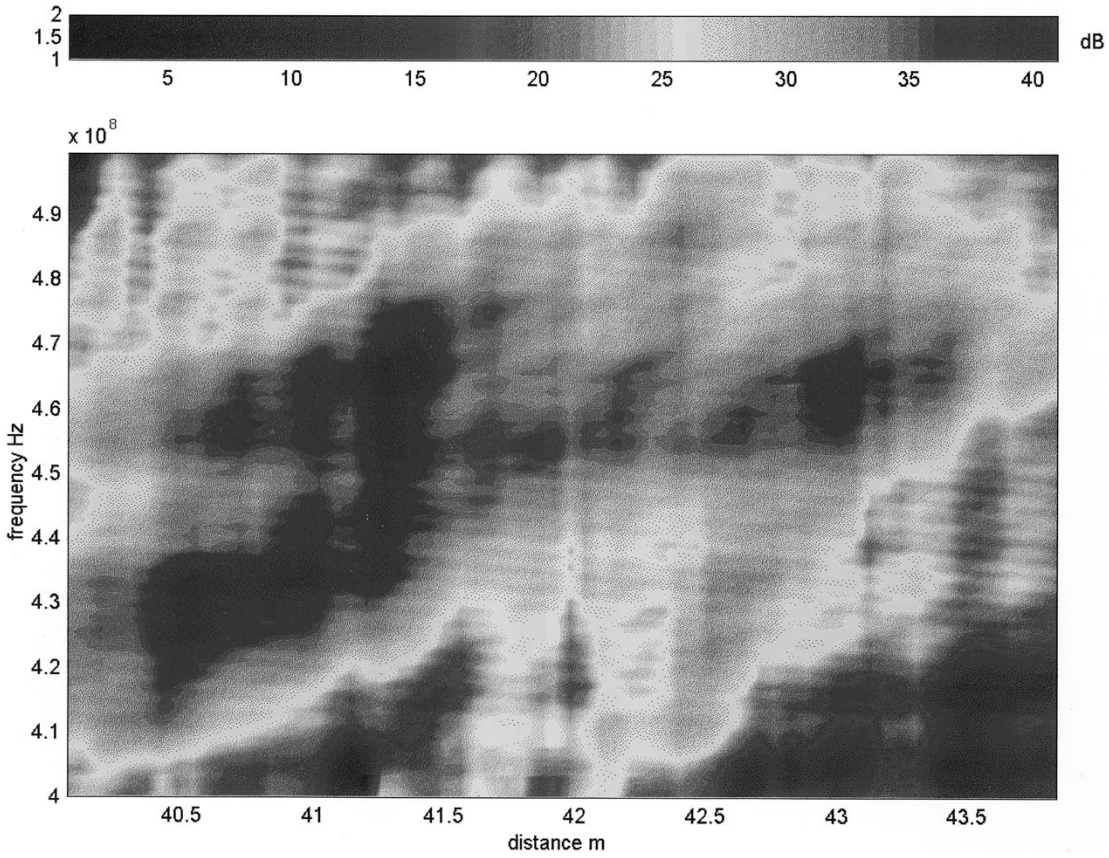

(a)

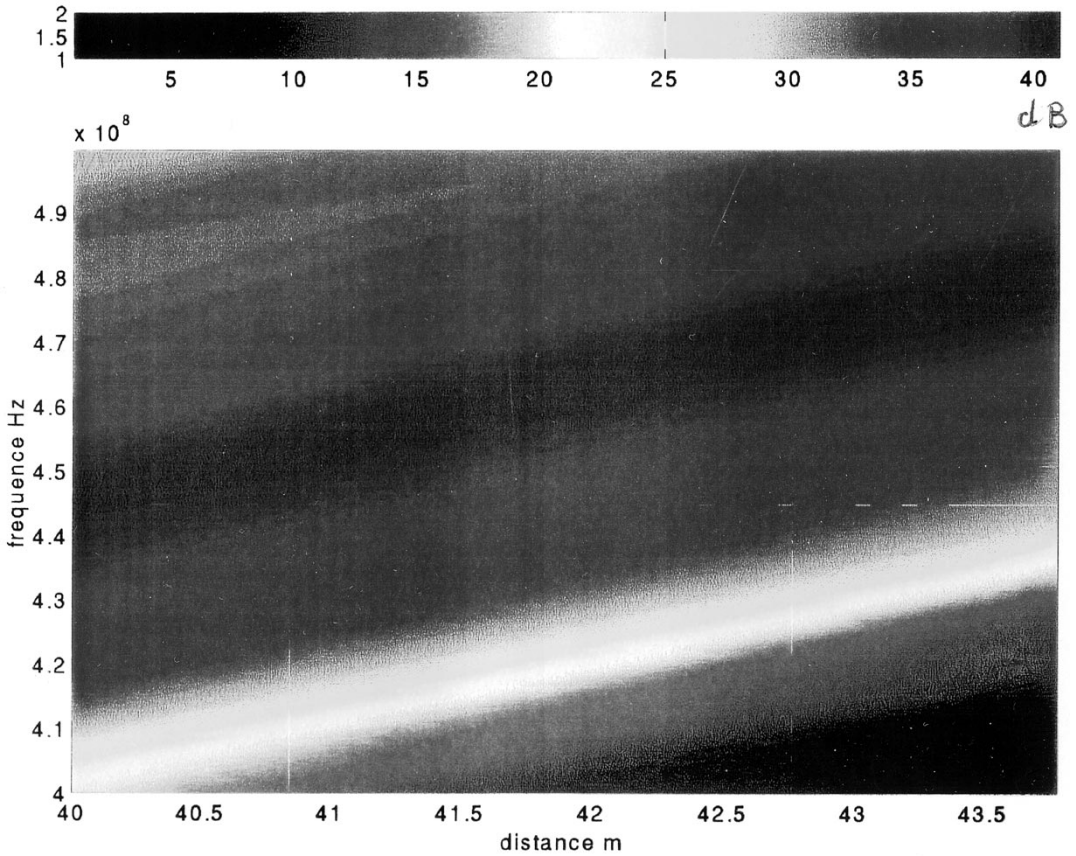

(b)

Fig. 3. Amplitude of the transfer function of the channel measured at a distance varying from 40 to 44 m from the transmitter. The color scale corresponds to a level expressed in decibels above an arbitrary level. Comparison between (a) experimental and (b) theoretical results.

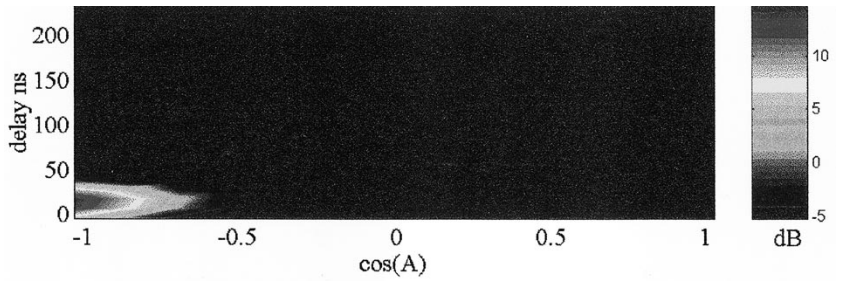

(a)

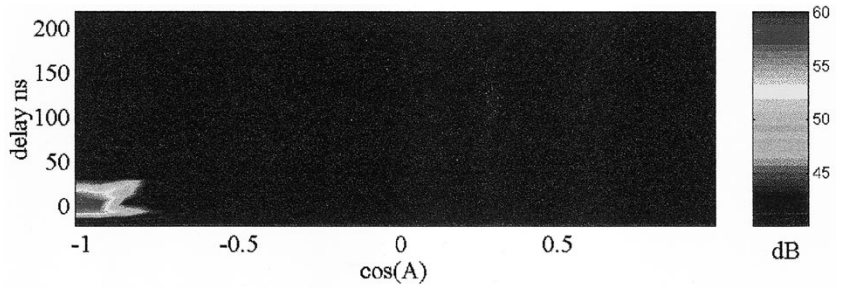

(b)

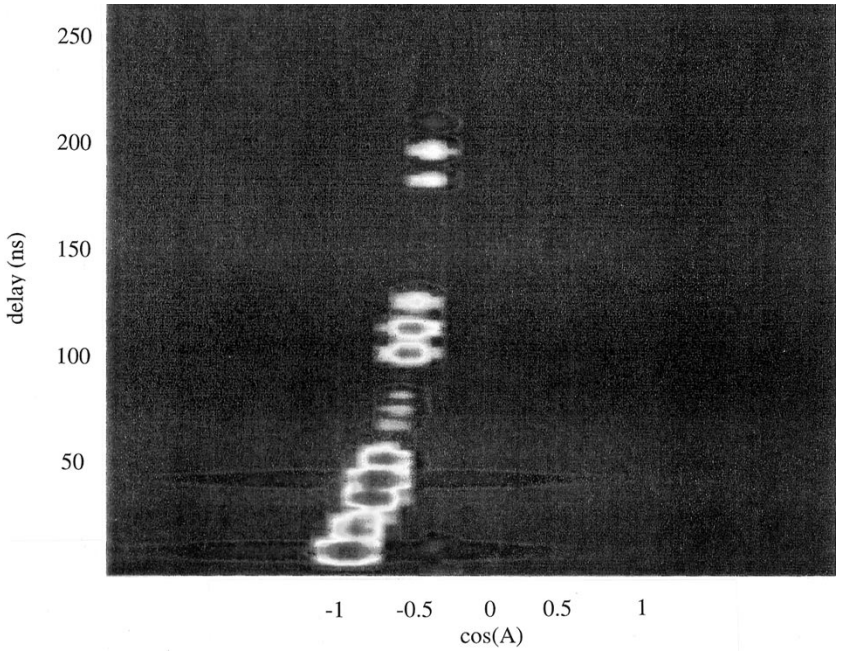

(c)

Fig. 4. Direction of arrival of the rays represented in the plane ($\cos A$-delay). (a) Theoretical results in the gallery. (b) Experimental results. (c) Theoretical results in a large tunnel.

to present the main theoretical and experimental results dealing with this application, the frequency band under consideration extending from 150 to 900 MHz.

If the lengths of the access galleries are not too important (few hundred meters), the natural propagation of the waves between a mobile transmitter and a fixed base station can also be used instead of installing a radiating cable. The first part of this paper will thus deal with the characterization of the propagation in a straight tunnel. If the longitudinal attenuation is an important criteria, the localization technique and the optimization of a digital communication also needs to have a good knowledge of the coherence bandwidth, of the delay spread, and of the direction

of arrival of the rays. In a second part, experimental results obtained in a room and pillars will be commented.

II. Propagation in a Straight Gallery

A. Theoretical Modeling

The EM wave propagation inside a mine tunnel can be theoretically studied by means either of a ray or of a modal approach. If the frequency is high enough, the tunnel behaves as an oversized waveguide with imperfectly conducting walls. In order to get analytical solutions through a modal theory, the geometry of the problem must be limited to circular or elliptical tunnels so that the air–ground boundary corresponds to a coordinate surface for which Helmoltz equation is separable. Nevertheless, approximate solutions have been proposed for a straight rectangular tunnel by Mahmoud and Wait [11], Mahmoud [12] and Emslie *et al.* [13]. Another approach is based on the ray theory by introducing reflection coefficients on the tunnel walls. Nevertheless, these coefficients can only be defined for incident plane waves on infinite plane interfaces, but they can be practically used for incident spherical waves when these are several wavelengths from the source and when the interface is only of finite extent. Assuming a straight tunnel of rectangular cross section, the components of the two Hertz potential vectors on each interface and associated with the incident and reflected waves, respectively, are related by a matrix equation whose terms are the reflection coefficients. The total field in the tunnel due to a given source being equal to the sum of ray contributions from all images added to that of the source, it can be shown that the resulting Hertz vector involves the product of all the reflection coefficient matrices associated with each image, taking the directional cosines of the ray into account [11]. The three electric field components are then derived from the resulting Hertz potential leading to a wave depolarization. However, if, for example, a vertical transmitting antenna is considered, it is interesting to know if this depolarization effect occurs only in the near range of the transmitter. A parametric study shows that the cross polarized field components become negligible beyond a distance equal to three times the largest dimension of the tunnel cross section [14] due to the fact that only waves incident on the walls with a grazing angle of incidence play a role at large distance. For the application described in this paper, this condition is always satisfied and an important simplification can be introduced in the propagation model by considering that the electric field remains vertically polarized, the transmitting antenna being a vertical dipole. The source images $S_{n,m}$ corresponding to rays reflecting n times on the horizontal walls and m times on the vertical ones, form a plane array perpendicular to the tunnel axis. Since the field is assumed to remain linearly polarized, the vector summation corresponding to the contribution of all the images becomes a scalar one and the field amplitude E is, thus, given by the following expression:

$$E = \sum_n \sum_m E_{n,m}(\,\mathrm{RTE})^n(\mathrm{RTM})^m \tag{1}$$

where RTE and RTM are the reflection coefficients on the horizontal and vertical walls, respectively, while $E_{n,m}$ is the direct field due to an image source $S_{n,m}$.

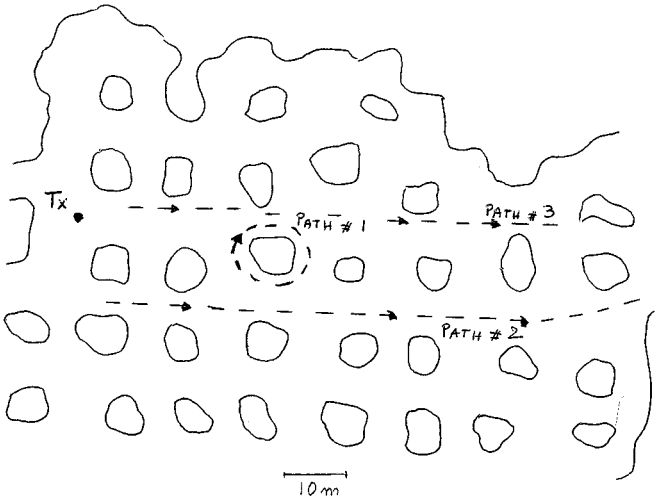

Fig. 5. Plane view of the room and pillars A, showing the position of the transmitting antenna (Tx), the receiver moving along the three paths noted #1, #2, and #3.

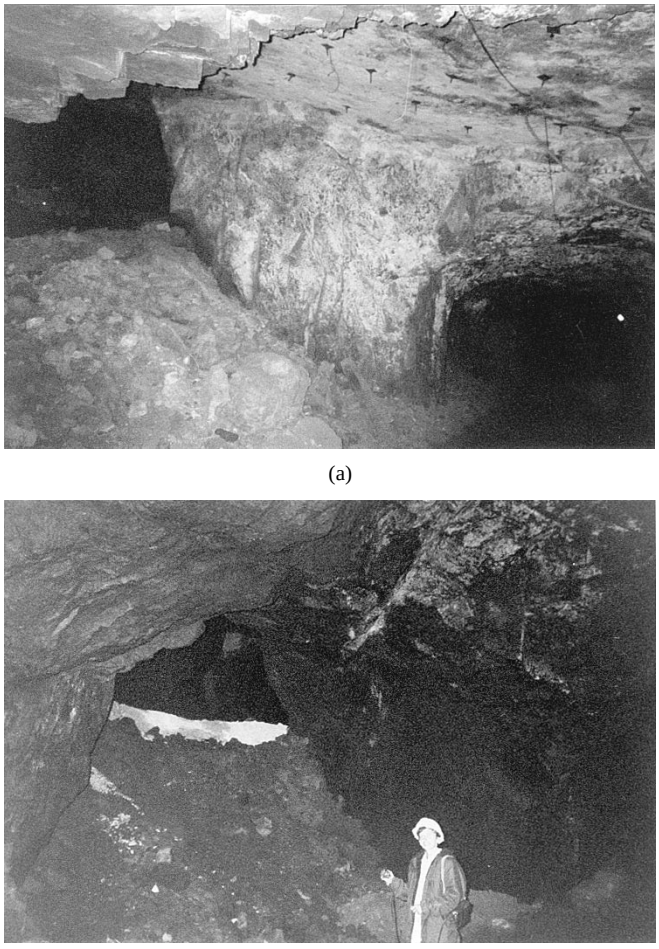

(a)

(b)

Fig. 6. Two typical views (a) and (b) of a partly refilled room and pillars.

If the gallery has an arbitrary shape, a ray-launching technique can be used, by discretizing the walls into planar facets. However, for long tunnels, this leads to numerical difficulties and the convergence is very tedious. In the following, the modeling will thus be made by only considering a straight rectan-

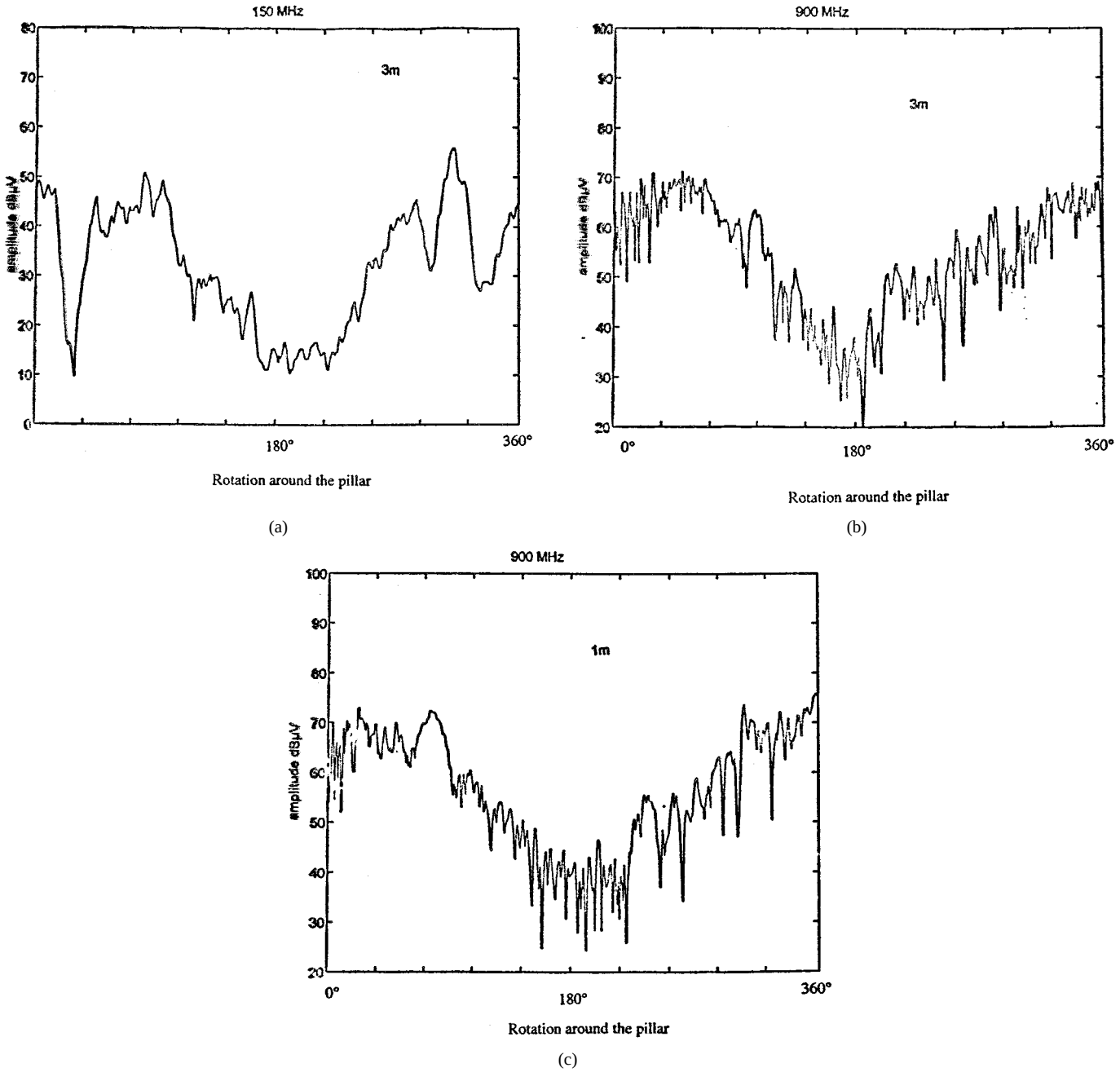

Fig. 7. Variation of the electric field amplitude when the mobile turns around a pillar (path #1). Curves (a) and (b) correspond to a frequency of 150 and 900 MHz, respectively, the receiving antenna moving at a distance of 3 m from the pillar. For curve (c) this distance has been reduced to 1 m, the frequency being 900 MHz.

gular tunnel and by calculating the electric field from (1). Indeed, in mines, many other parameters may play a leading part in the propagation such as the presence of obstacles (pipes, vents ...), the roughness of the walls and the imperfect shape which is also randomly variable along the gallery.

The reflection coefficients RTE and RTM in (1) and related to the parallel and perpendicular incidences, depend on the angle of incidence but also on the complex relative permittivity ε_r^* of the walls [15]. One can express this term as follows:

$$\varepsilon_r^* = \varepsilon_r + \sigma/j\omega\varepsilon_0 \tag{2}$$

ε_0 being the permittivity of free-space.

For a given frequency, an equivalent conductivity σ and a real permittivity ε_r are introduced. These terms are frequency dependent, but it is assumed that in the frequency range under consideration, between 450–900 MHz, their average values are equal to $\sigma = 10^{-2}$ S/m and $\varepsilon_r = 5$.

B. Field Attenuation

A first set of experiments have been carried out in a bauxite mine in Greece in one of the access galleries, 6 m high and 5 m wide. Its shape is more or less rectangular but the roughness is very important and the standard deviation of the average transverse dimensions is on the order of 50 cm. The transmitting and receiving antennas are half-wave vertical dipoles, the transmitting frequency being equal to 150, 450, and 900 MHz

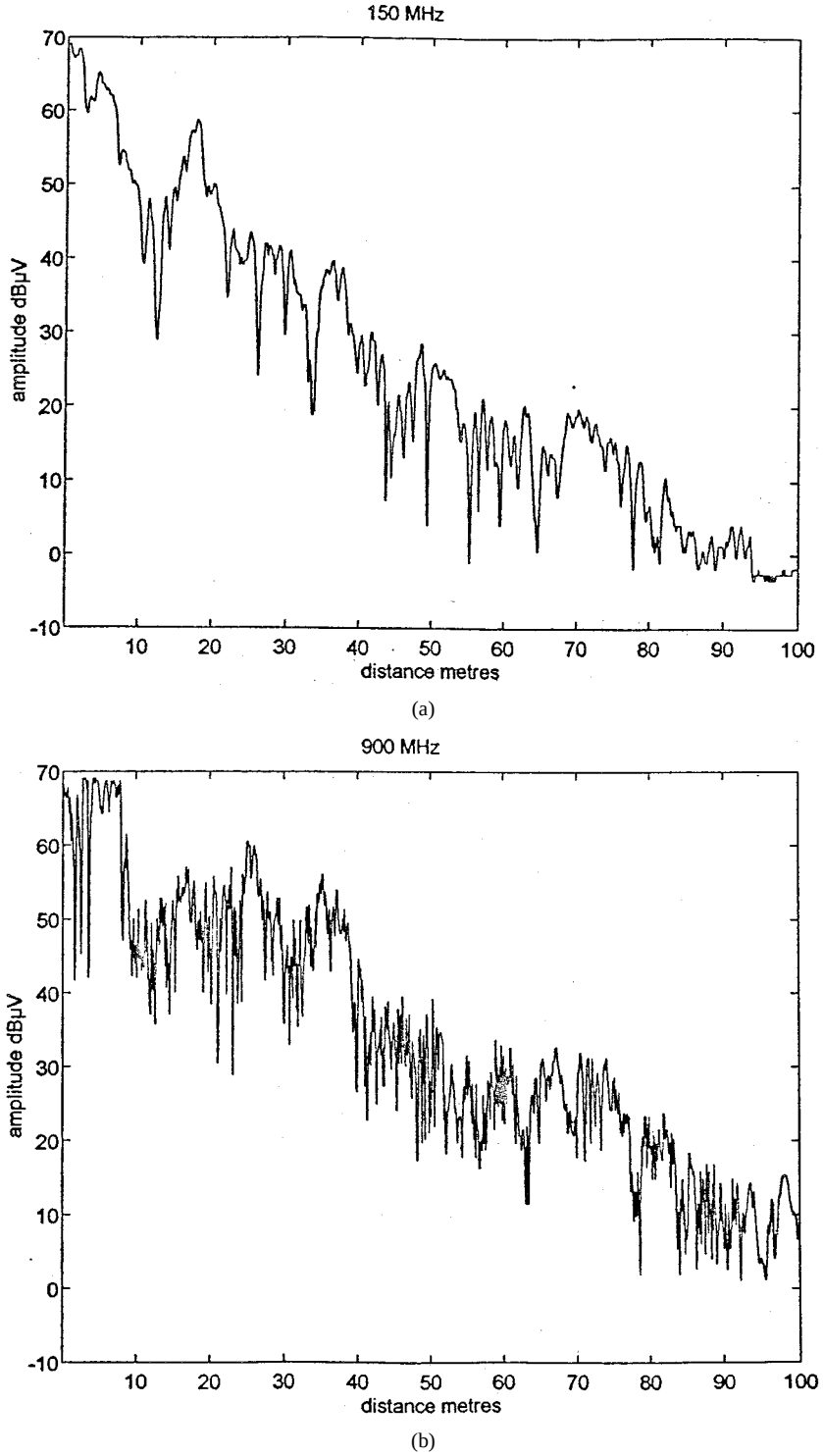

Fig. 8. Variation of the field amplitude along path #2 in the room and pillars A as shown in Fig. 5. (a) $f = 150$ MHz. (b) $f = 900$ MHz.

successively. At 150 MHz, the attenuation is prohibitive since it reaches 32 dB/100 m. For the two other frequencies, the variations of the received power, expressed in decibels above an arbitrary level are given in Figs. 1 and 2. The upper part of each of these figures corresponds to the theoretical results, the continuously decreasing curve being the contribution of the direct path to the total field.

The global shape of these curves shows that the mean variation of the signal amplitude versus the distance between the transmitter and the receiver can be divided into two zones. In the vicinity of the transmitter there are important fluctuations due to the contribution of all high-order modes excited by the transmitting antenna while, at a large distance, the low-order modes become dominant and the attenuation per unit length becomes much smaller.

For a frequency of 450 MHz, as shown in Fig. 1, an exponential decrease of the signal occurs beyond a distance of 150 m and the theoretical average attenuation is 4 dB/100 m, which must

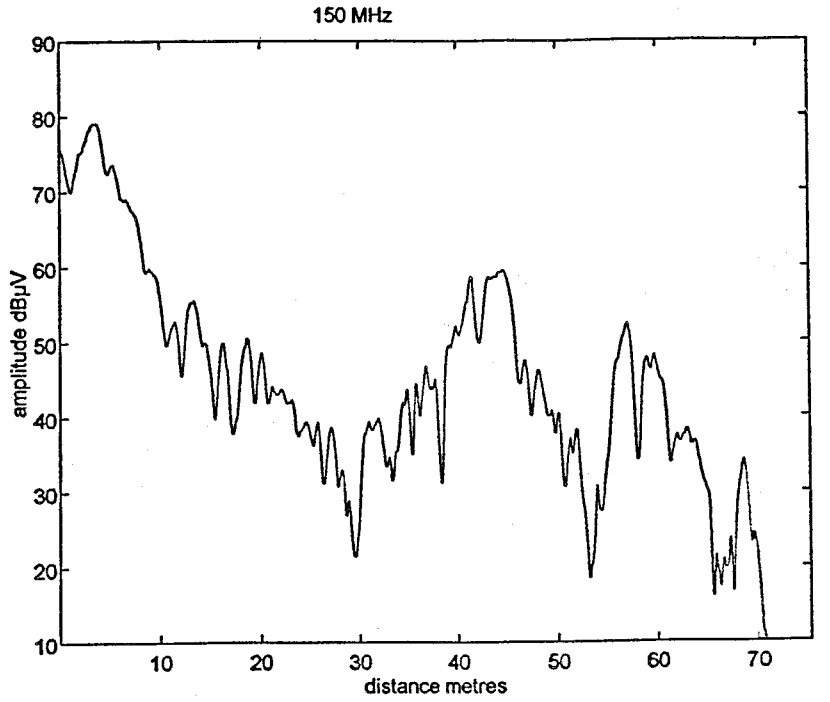

(a)

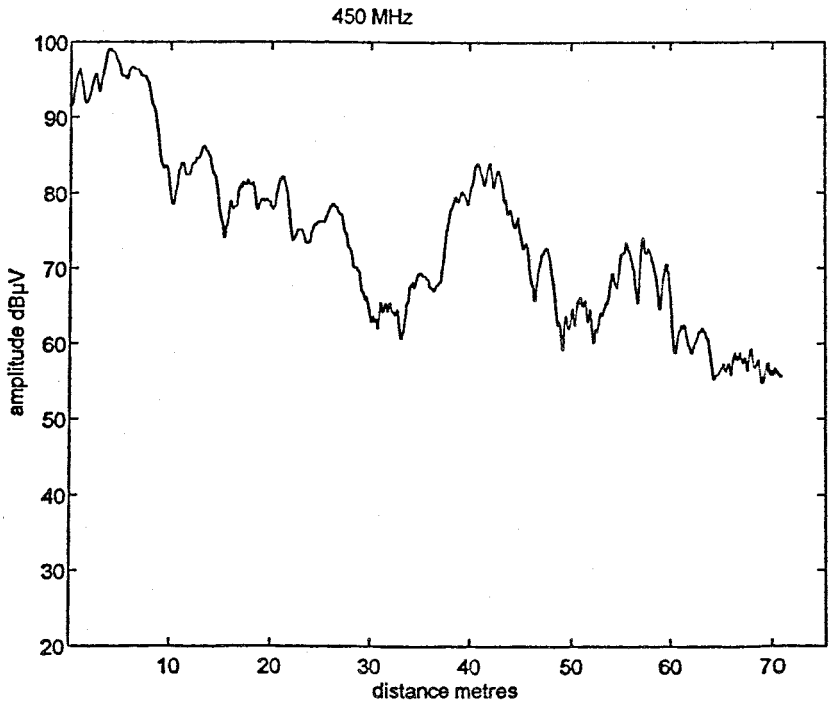

(b)

Fig. 9. Same as in Fig. 8, but in room B.

be compared to the much higher value of 9 dB/100 m deduced from the experimental curve. At 900 MHz, the theoretical and experimental attenuation between 10 and 250 m are 30 and 40 dB, respectively. It is difficult to deduce from the curves the attenuation per unit length far from the transmitter since between 300 and 500 m the attenuation becomes very small. Unfortunately, for practical reasons, it has not been possible to make measurements in this access gallery beyond this distance of 500 m. The highest attenuation of the measured signal can be explained by the important roughness and the approximate shape of the walls. Indeed, the reflection coefficients introduced in (1) are calculated assuming perfectly conducting plane surfaces and it was not possible to improve the theoretical model since the analytical approximate formulas giving the reflected field in the specular direction always suppose that the roughness is small in terms of wavelength [13].

It must be stressed that at higher frequencies and in much wider tunnels, the field distribution far from the transmitter

would present fast fluctuations, the high-order modes being not too much attenuated. Consequently, it was shown that the field distribution around the regression line and calculated along few kilometers in such tunnels follows a Rayleigh distribution [17].

C. Wide-Band Analysis

For a digital communication, parameters such as the impulse response and the coherence bandwidth of the channel must be determined to optimize, if necessary, the modulation scheme and the bit data rate. Furthermore, as previously mentioned, another objective of the project is to localize the mobile. The longitudinal position can be simply based on the principle of a time interval measurement: the base station sends, after a preamble and the identification of the mobile to be localized, a pulse which is reemitted by the mobile transmitter after a short but known delay [18]. A crucial point is thus to determine the spread of the impulse response, both in time domain and in angle of arrival, due to the multiple reflections on the walls.

In the access gallery, the transfer function of the channel has been measured versus frequency and distance transmitter (Tx)-receiver (Rx). First, the receiving antenna has been moved along a distance of 4 m, between 40 and 44 m from the transmitter. At each point, 6 cm apart, the transfer function, i.e., the received signal normalized to the transmitted signal, is determined in a frequency range extending from 400 to 500 MHz. The results are presented in Fig. 3(a) where each color corresponds to an amplitude, expressed in decibels, above an arbitrary reference level while the theoretical prediction is given in Fig. 3(b). One remarks both in theory and in experiment, a kind of translation symmetry in the distance-frequency plane. For example, in Fig. 3(b), a maximum value occurs at 40 m and for a frequency of 450 MHz and can be found again at 460 MHz slightly far away. This typical shape has been found whatever the distance Tx-Rx.

To interpret such a variation, one can start to determine the contribution of each image to the total field. The images distribution of the transmitting antenna in a transverse plane can be divided into series of horizontal lines, their spacing being related to the tunnel height. The horizontal line passing by the transmitter corresponds to multiple reflections on the horizontal plane only, while the others are associated with reflections on both the vertical and horizontal walls. Taking the values of the conductivity and permittivity of the walls into account, it appears that these walls behave, at 450 MHz, as a low-loss dielectric material. For a vertically polarized wave, the reflection coefficient on the horizontal walls decreases rapidly with the angle of incidence, because the Brewster angle is on the order of 70°. In a first approximation, one can thus only consider the contribution of the images situated on the horizontal line containing the transmitter and eventually, the first two lines situated on both sides. If the distance Tx-Rx is much larger than the tunnel width, the expressions of the delays between the rays and of the reflection coefficients can be simplified, using a second-order approximation. A straightforward calculation shows that the field amplitude remains constant in a given zone, as the ratio distance over frequency. A minimum or maximum field amplitude for a frequency f_1 at a distance x_1 will thus also occur at a slightly larger distance x_2, but for a frequency f_2 such that $x_1/f_1 = x_2/f_2$.

The coherence bandwidth, defined as the frequency separation at which the envelope correlation is 0.5, has been deduced from these curves and the theoretical and experimental values are 13 and 15 MHz, respectively. By applying a Fourier transform, the impulse response of the channel to a Gaussian pulse, 12 ns at midwidth, has been determined. It appears that the pulse is slightly broadened due to the contribution of the numerous rays, delayed from one another and, of course, the relative phase difference between these rays give rise to a distortion of the incident pulse. In order to quantify the spread of the impulse response, two quantities are usually introduced: the maximum excess delay and the delay spread. The first one is simply the longest delay relative to the first arriving pulse for which the amplitude of the received signal, referred to the first peak, is attenuated less than a given value often chosen equal to 20 dB. Since, in our case, it is not possible to clearly distinguish the successive pulses due to the finite bandwidth of the transmitting pulse, we have preferred to determine the delay spread σ_τ from the power delay profile $P(\tau)$. If $h(\tau)$ is the channel impulse response versus time $P(\tau)$ is found by taking the spatial average of $|h(\tau)|^2$ over a local area [19]. The delay spread is equal to the square root of the second central moment of $P(\tau)$ and is thus given by

$$\sigma_\tau^2 = \frac{\int_0^\infty (\tau - \tau_m)^2 P(\tau)\, d\tau}{\int_0^\infty P(\tau)\, d\tau} \tag{3}$$

where τ_m is the mean propagation delay, given by

$$\tau_m = \frac{\int_0^\infty \tau P(\tau)\, d\tau}{\int_0^\infty P(\tau)\, d\tau}. \tag{4}$$

The statistical study shows that for this environment, the mean delay spread is on the order of 10 ns. It means that despite the multiple reflections on the walls, the difference in time between rays contributing significantly to the received power remains small. The precision of a localization method in a mine gallery, based on a time measurement between a transmitting and a receiving pulse, will thus not suffer on the effect of multipath propagation, at least if the expected accuracy is on the order of few meters. Indeed, we are not faced with the case of a first pulse of small amplitude followed by a succession of large echoes. Another way to check this result is to determine the direction of arrival of the rays.

D. Direction of Arrivals

The spread of the angle of arrival of the successive rays as a function of time delay and amplitude is determined from the complex impulse response at successive positions of the receiver. Fig. 4(a) and (b) shows the map of the directions of arrival at a distance of 40 m from the transmitter deduced from experimental and theoretical results, respectively. The abscissa is the cosine of the angle A between the tunnel axis and the rays, the ordinate is the excess time delay normalized to the first received pulse, while the amplitude of the signal, expressed in decibels, is given by the color scale. It clearly appears that most

TABLE I
AVERAGE ATTENUATION VERSUS THE DISTANCE BETWEEN A REFERENCE POINT, 10 m AWAY FROM THE TRANSMITTING ANTENNA, AND A MOBILE ANTENNA, IN VARIOUS ROOMS AND PILLARS

Frequency	150 MHz	450 MHz	900 MHz
Distance			
20m	40 dB	20 dB	20 dB
50m	50 dB	40 dB	30 dB
70m	60 dB	45 dB	50 dB
100m	75 dB	65 dB	60 dB

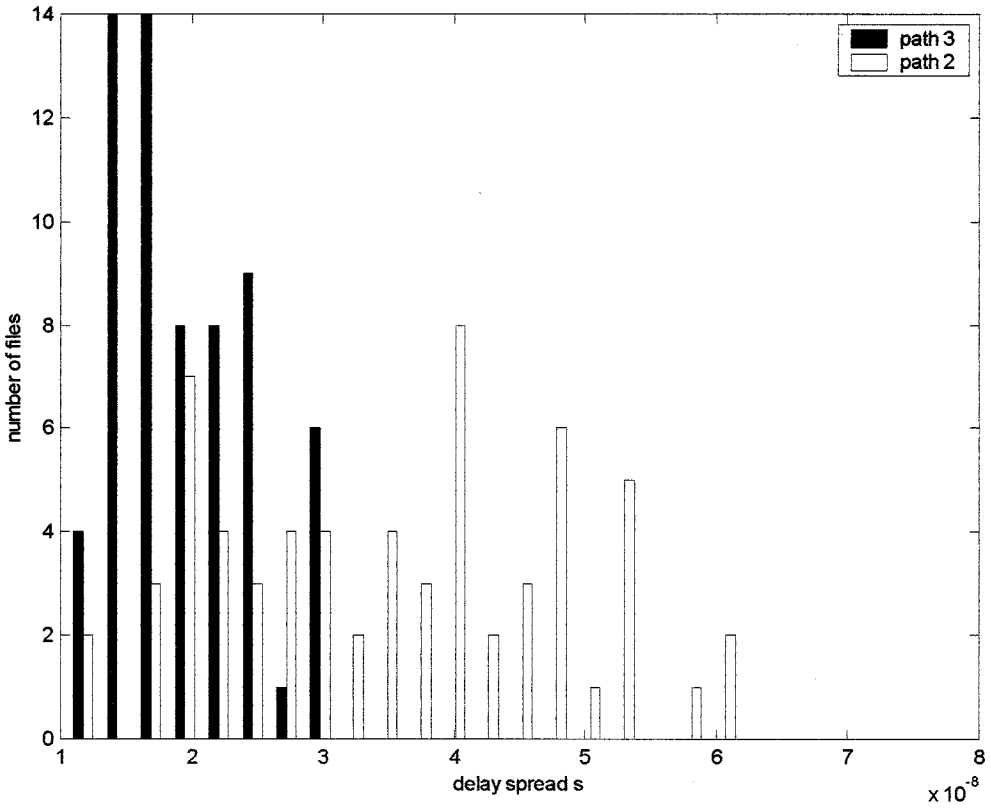

Fig. 10. Distribution of the delay spread measured along two paths in a room and pillars. Along path 3, the receiver is in the line of sight of the transmitter, while, along path 2, the direct path is obstructed.

of the energy comes from a direction corresponding nearly to the tunnel axis, i.e., to a cosine equal to -1 or an angle of 180°. In such a gallery, the spread angle can thus be neglected even at short distance from the transmitter. To clearly point out an angle distribution at this distance, it would be necessary to consider much wider galleries, an illustration being given in Fig. 4(c) for a tunnel 13 m wide and 8 m high. In this case, it appears that reflected pulses arriving with an angle of incidence of 60° referred to the tunnel axis and a mean delay of 100 ns, still contribute to the total field, their maximum amplitude being 12 dB less than the one of the most energetic pulse.

In conclusion of this first part, it has been shown that the wall roughness and a tunnel cross section whose geometry is variable from one point to another one, produce an important increase of the longitudinal attenuation. Nevertheless, all the wide-band characteristics of the channel such as coherence bandwidth, delay spread, and spread of the angle of arrival of the rays can still be satisfactory predicted from a simple analytical model. Despite the distortion of the emitted pulse, the mobile localization can thus be achieved owing to the knowledge of the instant at which the signal amplitude exceeds a given threshold.

TABLE II
AVERAGE DELAY SPREAD AND COHERENCE BANDWIDTH IN DIFFERENT ENVIRONMENTS

Configuration	Line of sight	Non line of sight Room A	Non line of sight Room B	In gallery
Delay spread	19 ns	26 ns	42 ns	5 ns
Coherence bandwidth	4.3 MHz	2.8 MHz	2 MHz	15 MHz

III. PROPAGATION IN ROOM AND PILLARS

To localize a mobile in a room and pillars, the basic idea is to put at least two fixed antennas in the room and, by measuring once again the delay of the received pulse reemitted by the mobile antenna, to deduce its position by triangulation. For this application, as well as for data transmission, a narrow-band and wide-band analysis has been made.

A. Narrow-Band Analysis

It must first be recalled that a so-called room and pillars is not necessarily horizontal and its height at any point depends on the thickness of the ore deposit. Furthermore, its configuration is continuously changing, part of the room being filled up. A typical plane view of such a room called room A (in the following) is shown in Fig. 5. The mean height is about 6 m and the thickness of a pillar is on the order of 4–6 m, its shape being more or less squared or circular. Photos showing part of the environment are given in Fig. 6. Due to the configuration of a room, it is illusive to think that a global modeling could bring quantitative information. A lot of experiments has thus been made in various rooms.

At first, it could be of interest to know the attenuation, near the transmitter due to pillars intercepting the direct ray. In Fig. 5, the position of the transmitter is indicated by $\ll$Tx$\gg$ and the receiver is moved along path #1 by making a complete rotation around a pillar at a distance either of 3 or of 1 m from its walls, part of the path being in the line of sight of the transmitter. Curves (a) and (b) in Fig. 7, correspond to a distance of 3 m and have been plotted for the two extreme frequencies under consideration: 150 and 900 MHz. The relative field amplitudes, expressed in decibels above an arbitrary level, of course reach their maximum values when the receiver is in the line of sight of the transmitting antenna. In the deep shadow region, the attenuation is about the same whatever the frequency, on the order of 35–40 dB. If the diffraction phenomena by the edges of the pillar would be dominant, a decrease of the received signal must be observed at 900 MHz. The same kind of variation would occur if the pillar is considered as a smooth cylinder supporting creeping waves. The influence of the other pillars and walls giving rise to diffuse reflections is thus, by far, the most important phenomena. This can also be checked in Fig. 7 curve (c), plotted again for a displacement of the antenna around the pillar for a frequency of 900 MHz, but at a distance of only 1 m from the pillar walls. Indeed, by comparing curves (b) and (c), it appears that the additional attenuation due to the masking effect is independent on the position of the receiving antenna behind the pillar.

The next step is to determine the mean longitudinal attenuation versus frequency. Various positions of the transmitting antenna have been considered, and furthermore, measurements were made in various rooms in order to get reliable results. As an example, curves (a) and (b) in Fig. 8 represent the field amplitude variation along path #2, about 100 m long, shown in Fig. 5, and for two frequencies: 150 and 900 MHz. The longitudinal attenuation is smaller at 900 MHz, but not in a so large proportion as in the case of propagation in a straight gallery. Another example is shown in Fig. 9 in another room B, having a much more complex geometry. The curves, plotted for a frequency of 150 and 450 MHz exhibit the same variation with, however, a smaller attenuation at 450 MHz.

Table I summarizes the average values of the attenuation, measured along various paths and in different rooms, between a reference point situated at 10 m from the transmitting antenna and in its line of sight and areas situated between 20 m and 100 m from this point.

The difference in the results obtained at 450 and 900 MHz is not significant and, for practical reason in the system design, a carrier frequency of 450 MHz was chosen. Therefore, the wide-band analysis presented in the next paragraph mainly concerns this frequency range.

B. Wide-Band Analysis

The transfer function of the channel between the transmitting and receiving antennas has first been determined by measuring at many points in the rooms, the amplitude and phase of the received signal in a frequency band extending from 400 to 500 MHz.

Fig. 10 gives the histogram of the delay spread, which has been deduced from these measurements in room A, for points distributed on two paths 100 m long, the receiving antenna being situated either in the line of sight of the transmitter, path 3, or not, path 2, as shown in Fig. 5. The total number of stored files along each path is 64. In the first case, it appears that about 60% of the values are between 15 ns and 20 ns, the mean delay spread being 19 ns. On the contrary, for an obstructed path, the values are more spread and larger since they extend from 15 ns up to 65 ns with a mean of 42 ns.

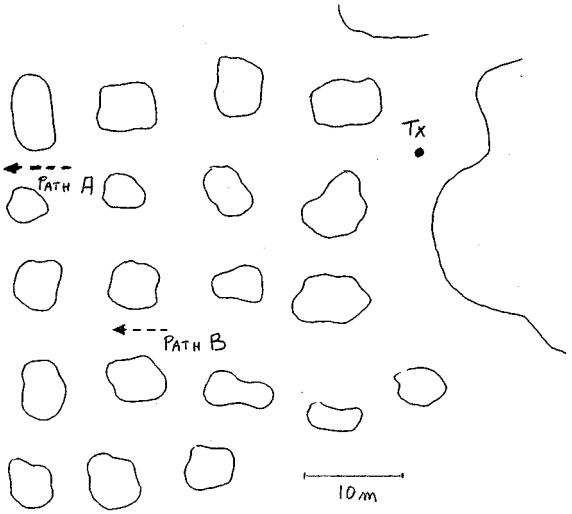

(a)

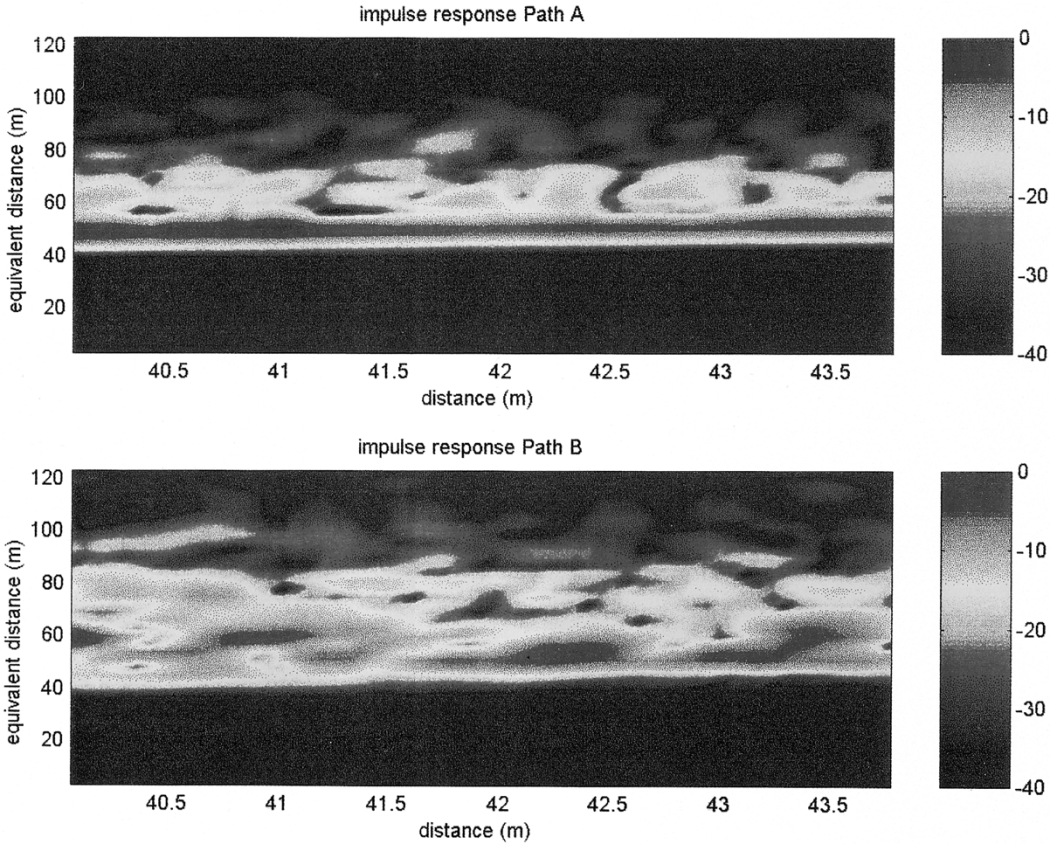

(b)

Fig. 11. Impulse response of the channel. (a) Geometrical configuration showing the position of the transmitter (Tx) and the two paths A and B whose axes are the successive references for measuring the direction of arrivals. (b) Impulse response versus the position of the receiver. The unit of the ordinate axis has been converted from time to equivalent distance.

To minimize the effect of the multipath propagation giving rise to local deep fadings, various techniques such as the spread spectrum, can be used. For optimizing the various parameters of the link, it is also important to determine the coherence bandwidth in various configurations. The results, summarized in Table II, have been obtained in two different rooms A and B. The structure of room B is quite more complex than in room A, where the previous results have been obtained. Indeed, in this room, the thickness of the ore deposit is continuously varying and, thus, the height of the room accordingly. Furthermore, the pillars have a quite irregular structure, both in shape and thickness, and they are randomly distributed. Finally, the room is partly refilled and the floor is not flat at all. As a comparison, the results obtained in an access gallery are also recalled.

It appears that in a mine environment, the channel characteristics vary considerably from an area to another one and the typical values given above may be introduced in a channel model to predict the performance of the link.

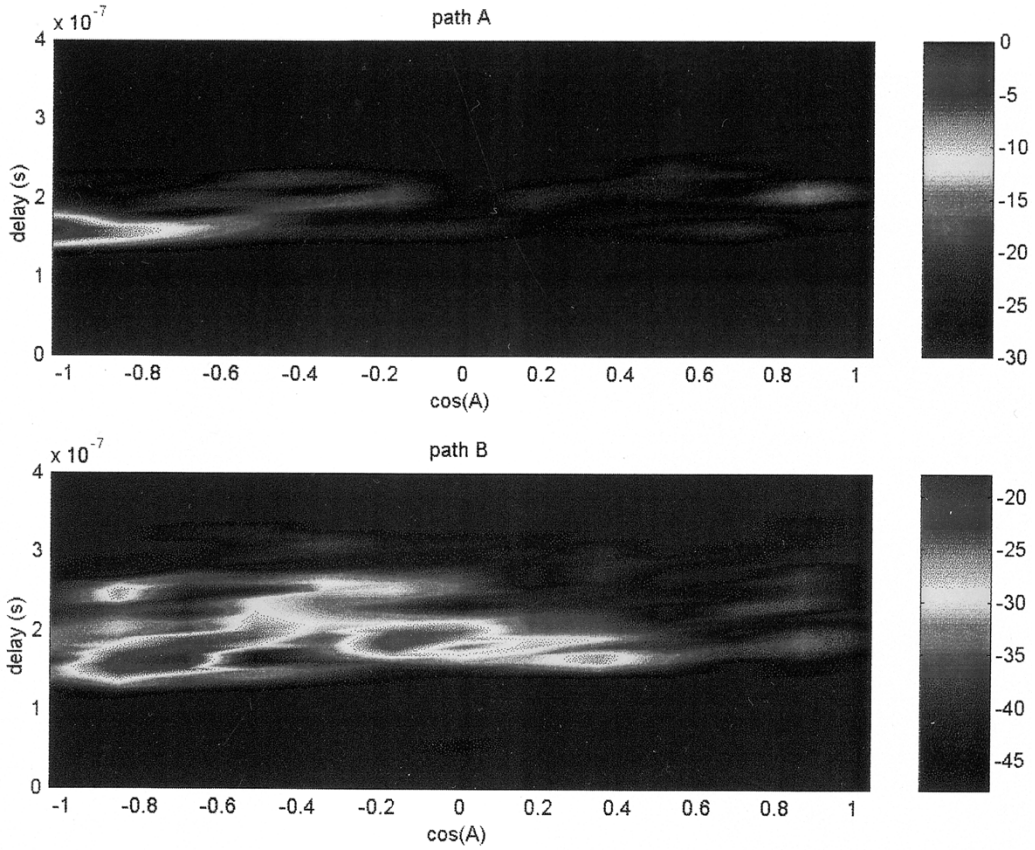

Fig. 12. Amplitude of the impulse response versus both the direction of arrival and the delay of the EM waves.

The other aspect concerns the localization of a miner or of a mobile in the room. It can be done, owing to the same principle as in a straight gallery by measuring the time interval between the pulse transmitted by a fixed antenna and the received pulse,which has been reemitted by the mobile transmitter. Of course, at least two fixed antennas are needed to determine the position in the horizontal plane. To get an idea of the error introduced by the multipath propagation, another set of experiments has been carried out. The transmitter (Tx) was put at the entrance of a room, near the end of the access gallery. Two different configurations have been tested in order to be or not in the line of sight of the fixed antenna, acting in this case as a transmitting one. The first path, called path A in Fig. 11(a), is situated between 40 and 44 m, in the line of sight of the transmitting antenna, while the second one, path B, is situated at the bottom of an important slope and the direct path is always obstructed.

The amplitudes of the impulse response are shown in Fig. 11(b). The abscissa corresponds to the true distance between the transmitter and the receiver, while the ordinate is the delay of transmission, which has been converted into meters, assuming that the waves propagate at the velocity of light. For a given abscissa, the impulse response is represented owing to a color scale, each color referring to an amplitude expressed in decibels above an arbitrary level. If we consider the path A, it clearly appears that the first received pulse has a maximum amplitude and is thus clearly identified, even if the multiple echoes on the various pillars and walls broaden the incident pulse and give rise to a series of other delayed pulses. Their extent, converted in meters, is between 40 and 60 m if an attenuation of 15 dB, referred to the highest peak, is considered. When the direct path is obstructed, the maximum amplitude of the pulses does not necessarily correspond to the shortest path as it appears from Fig. 11(b), path B. Furthermore, this peak amplitude may considerably vary from one point to another one, even situated in the same area and the impulse response is much wider. It is thus important to base the localization system on the detection of a threshold level, for example 15 dB above noise. Indeed, the advantage of an underground mine is that all the EM disturbances present above the ground surface are strongly attenuated and that the noise due to the electric engines such as vents, decreases rapidly above few hundred of kilohertz.

Another interesting point concerns the directions of arrival of the rays. They are deduced from the complex impulse responses of the channel measured at many points, few centimeters apart. These points are situated along a straight line and, in this two-dimensional approach, the angle of arrival is defined, as previously, as the angle A between a ray and the axis of displacement of the receiving antenna. Fig. 12 shows the results in the plane ($\cos A$, delay), the amplitude of the received signal, expressed in decibels, being given by the color scale. Along path A, there is only one significant contribution corresponding to the line of sight, the receiver moving away from the transmitter. For path B, in the absence of the direct ray, there are two main contributions, one arriving with an angle of about 140° ($\cos A = -0.8$) and the other one at 100° ($\cos A = -0.15$). The first one nearly

corresponds to the line joining the transmitter and the receiver since, as it appears in Fig. 11(a), the receiver was not moving in the direction of the Tx-Rx axis, but along a path making a angle of about 130° with this axis. From additional measurements, it thus appears that even if the direct path is obstructed, the localization of the mobile can be still achieved by detecting the time when the signal level exceeds a threshold value, 15 dB above noise. In this case, the expected precision of the localization is on the order of 5 m.

IV. Conclusion

The theoretical modeling in a straight rectangular tunnel has been presented and a good agreement was obtained between theoretical and experimental results for trials made in a road tunnel. However, in mines, the imperfect shape of the walls as well as their important roughness lead to an important increase of the longitudinal attenuation which can reach 9 dB/100 m at 450 MHz.

The configuration of a room and pillars is so complicated that only an experimental approach has been made. The average characteristics of the channel have been determined such as the coherence bandwidth and the delay spread of the impulse response. These values are, of course, strongly dependent on the various types of areas within the mine but can be introduced in a channel model to optimize the telecommunication scheme. Finally, it appears that the localization of a mobile, based on a time interval measurement, can be made with an expected accuracy of 5 m, even in a room and with pillars.

Acknowledgment

The authors would like to thank the other members of the consortium and the miners of Bauxite Parnasse, Greece, for their help during the experiments.

References

[1] A. G. Emslie *et al.*, "Use of auxiliary dedicated wire as a mean of aiding carrier current propagation on a trolley wire/rail transmission line," in *Proc. Electromagn. Guided Waves Mine Environments Workshop*, J. R. Wait *et al.*, Ed., Boulder, CO, Mar. 1978, pp. 26–41.

[2] P. Delogne, "Basic mechanisms of tunnel propagation," *Radio Sci.*, vol. 11, pp. 295–303, 1976.

[3] D. A. Hill and J. R. Wait, "Excitation of monofilar and bifilar modes on a transmission line in a circular tunnel," *J. Appl. Phys.*, vol. 45, pp. 3402–3406, 1974.

[4] J. R. Wait and D. A. Hill, "Guided electromagnetic waves along an axial conductor in a circular tunnel," *IEEE Trans. Antennas Propagat.*, vol. AP-22, pp. 627–630, July 1974.

[5] D. B. Seidel and J. R. Wait, "Transmission modes in a braided coaxial cable and coupling to a tunnel environment," *IEEE Trans. Microwave Theory Tech.*, vol. MTT-26, pp. 494–499, July 1978.

[6] J. R. Wait and D. A. Hill, "Propagation along a braided coaxial cable in a circular tunnel," *IEEE Trans. Microwave Theory Tech.*, vol. MTT-23, pp. 401–405, May 1975.

[7] D. A Hill and J. R. Wait, "Electromagnetic theory of the loosely braided coaxial cable: Numerical results," *IEEE Trans. Microwave Theory Tech.*, vol. MTT-28, pp. 326–331, Apr. 1980.

[8] M. Liénard *et al.*, "Theoretical and experimental study of radio coverage in tunnels using radiating cables," *Ann. Telecommun.*, vol. 49, pp. 143–153, 1994.

[9] M. Liénard and P. Degauque, "Wideband analysis of propagation along radiating cables in tunnels," *Radio Sci.*, vol. 34, pp. 113–122, 1999.

[10] P. Delogne, "EM propagation in tunnels," *IEEE Trans. Antennas Propagat.*, vol. 39, pp. 401–406, Mar. 1991.

[11] S. F. Mahmoud and J. R. Wait, "Geometrical optical approach for electromagnetic wave propagation in rectangular mine tunnels," *Radio Sci.*, vol. 9, pp. 1147–1158, 1974.

[12] S. F. Mahmoud, *Electromagnetic Waveguides*, ser. Inst. Elect. Eng. EM Ser. 32. Stevenage, U.K.: Peter Peregrinus, 1991.

[13] A. G. Emslie, R. L. Lagace, and P. F. Strong, "Theory of the propagation of UHF radio waves in coal mine tunnels," *IEEE Trans. Antennas Propagat.*, vol. AP-23, pp. 192–205, Feb. 1975.

[14] M. Liénard, P. Lefeuvre, and P. Degauque, "Remarques concernant le calcul de la propagation d'ondes haute fréquence en tunnel," in *Ann. Télécommun.*, Mar. 1997, pp. 529–533.

[15] *Electromagnetic Waves in Stratified Media*, 1962.

[16] P. Mariage, M. Liénard, and P. Degauque, "Theoretical and experimental approach of high frequency waves in road tunnels," in *IEEE Trans. Antennas Propagat.*, vol. 42, Jan. 1994, pp. 75–81.

[17] M. Lienard and P. Degauque, "Propagation in wide tunnels at 2 GHz: A statistical analysis," *IEEE Trans. Veh. Technol.*, vol. 47, pp. 1322–1328, Nov. 1998.

[18] M. Maignan and J. Boby, "Procédé et Système de Localization," Inst. Nat. de la Propr. Indus., Paris, patent 5 315 170F, 1993.

[19] T. S. Rappaport, *Wireless Communications, Principles and Practice*. Englewood Cliffs, NJ: Prentice-Hall, 1996.

Martine Liénard was born in Cambrai, France, on October 22, 1964. She received the M.S. and Ph.D. degrees from the University of Lille, Lille, France, in 1988 and 1993, respectively.

In 1990, she joined the Laboratoire de Radiopropagation et Electronique, University of Lille, where she is presently a Maître de Conférences. Her current research deals with both the theoretical and experimental prediction of propagation characteristics in confined areas using either radiating cables or natural propagation and the optimization and performances of modulation and diversity schemes such as orthogonal frequency division multiplexing and spread-spectrum techniques for wireless local area network and power line communications.

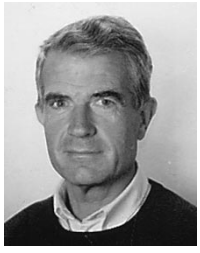

Pierre Degauque (M'76) was born in Lille, France, on September 19, 1946. He received the M.S. and Ph.D. degrees from the University of Lille, Lille, in 1966 and 1970, respectively, and the Engineering degree from the Institut Supérieur d'Electronique du Nord, Lille, in 1967.

Currently, he is a Professor and Head of the Laboratoire de Radiopropagation et Electronique, University of Lille . Since 1967, he has been working in the field of electromagnetic wave propagation and radiation from various antenna configurations. He was involved in research on radiation of antennas situated in absorbing media for geophysical applications. His primary interest is now in radio propagation in confined areas, mines, and tunnels based either on radiating cables or on natural propagation. He is also active in research on electromagnetic compatibility, including wave penetration into structures and coupling to transmission lines.

Dr. Degauque is Vice Chairman of URSI Commission E (electromagnetic noise and interference).